QUASI-FRAGILE AND FRAGILE FRACTURE BEHAVIOR WITH THE COHESIVE SURFACE METHODOLOGY

Luciani Neves Lens[a,b], Eduardo Bittencourt[b], Virgínia Maria Rosito d'Avila[b]

[a]Centro de Ciências Exatas e Tecnológicas, Universidade Estadual do Oeste do Paraná, Campus de Cascavel, Rua Universitária 2069, Cascavel, PR, Brazil, lnlens@unioeste.br, http://www.unioeste.br
[b]Centro de Mecânica Aplicada e Computacional, Univesidade Federal do Rio Grande do Sul, Avenida Osvaldo Aranha, 99, Porto Alegre, RS, Brazil, bittenco@cpgec.ufrgs.br, vichy@ufrgs.br, http://www.ppgec.ufrgs.br/Cemacom

Keywords: Fracture Mechanics, Concrete, Cohesive Surface Methodology, Finite Elements.

Abstract. The cohesive surface methodology is probably the most used in recent Fracture Mechanics researches (see Needleman, A., A continuum model for void nucleation by inclusion debonding, J. Appl. Mech., 54:525-531, 1987). This methodology is characterized by two parameters, the energy fracture and a characteristic length (or maximum stress at crack tip), and has been used to model fragile and ductile material satisfactorily. On the other side, quasi-fragile materials (as concrete) also need two fracture parameters to be characterized, depending on the used methodology. Then concrete seems to be a material that can be model by the above mentioned methodology. However, concrete is a strong heterogeneous material and its behavior depends on mortar properties and aggregate size and shape. Also, a factor that complicates the analysis of this material is the fact that the fracture process is accompanied by intense micro-cracking and bridging of main cracks. Recent numerical applications to concrete show that not only these two parameters are sufficient to correctly model its fracture process, but also other parameters as the shape of crack tip stress - crack opening function.

In this paper a discussion about the relations among all the above mentioned parameters is introduced and suggestions are raised on how to capture the quasi-fragile behavior with the cohesive surface methodology. The effect of micro-cracking is addressed as well as the effect of the shape of the stress-opening interface curve. A three-point bending beam is used as a numerical experimentation and compared to experimental results. The results show that micro-cracking and unloading shape of the stress-opening interface curve are variables as important as maximum stress at crack tip. Also it is shown that the original shape proposed by Needleman can not be used in quasi-fragile material when micro-cracking is considered. However, the methodology works quite well when only one main crack is considered, at least for the material and boundary conditions tested here.

1 INTRODUCTION

Maybe the biggest challenges to create a fracture model to concrete are the complex dissipative phenomena that occur in the so called process zone. In this zone micro-cracks are created as well as bridges between them. Bridging is a phenomenon frequently related to aggregate presence (see Van Mier, 1997 and Shah et al. 1995). The result is a long tail in the load-displacement curve, after peak value. Micro-cracks can produce a shielding effect for the main crack that may increase toughness when compared to a pure brittle material (Ortiz, 1988). The immediate consequence is the impossibility of the use of the Linear Elastic Fracture Mechanics (LEFM) to model concrete.

Experimental studies relating fracture mechanics to concrete were pioneered by Kaplan (1961). Then several experiments have shown that fracture toughness increases with the aggregate size, possibly because of the bridging effect. The first to show that was Naus and Lott (1969) and were subsequently corroborated by Strange and Bryant (1979), Petersson (1980) and Santos et al. (1998), only to cite a few. Guinea et al. (2002) showed this trend only for a particular shape of aggregate and focused also their study in the mortar-aggregate interface.

A long list of application of fracture mechanics models applied to concrete can be found. The paper by Ingraffea (1984), Rots (1988), van Mier (1997), Tijsens et al. (2000), etc are examples of interesting numerical studies in the field. When there is not a predominant crack, such as in reinforced concrete, the idea of the fictitious crack model introduced by Hilleborg et al. (1976) can be used. In this case only the bulk constitutive equation is modified adding an unloading part after peak stress. The unloading part is related to fracture energy. This model can be classified as a damage model rather than a fracture mechanics model because cracks do not need to be discrete.

The model presented here is the cohesive surface model in the same way proposed by Xu and Needleman (1994). Another attempt to use cohesive surface model to concrete can be also found in Tijssens et al. (2000). The way Xu and Needleman proposed their constitutive law is very attractive because two material parameters are necessary to define fracture properties, as in concrete (see for instance Shah et al. 1995). Finally the proposed law should work for fragile-elastic material as well as for ductile-plastic materials. In this paper is explored the possibilities of the original model proposed by Xu and Needleman for concrete applications, usually classified as a quasi-fragile material.

According de Borst et al. (2006), while for ductile fracture the most import factor of the cohesive surface model seem to be the tensile strength, for quasi-fragile material, where micro-cracking plays an important factor, the shape of the stress-opening relation of the crack appears to be more significant. Chandra et al. (2002) also claim that shape of stress-opening relation can not be neglected in the analysis of quasi-fragile materials. Finally, Tjssen et al. (2000) reported that fracture path of concrete is mainly determined by the initial slope of softening of the cohesive law. A preliminary study about the effect of unloading shape is also presented in this work.

In section 2 the interface constitutive law is presented as well as its implementation in a Finite Element Method (FEM) context. In section 3 a short review of the CEB (Comité Euro-International du Béton, 1993) definitions of concrete properties is presented. In section 4 a simulation of three point bending case is presented and the capabilities of the theory is explored to simulate different types of concrete. Discussion and conclusion remarks are presented in section 5.

2   THE COHESIVE SURFACE METHODOLOGY

The fracture behavior is here analyzed using the FEM together with cohesive elements (Needleman, 1987 and Xu and Needleman,1994) throughout the whole continuum. Considering an interface opening $\{\Delta\}$ in bi-dimensional problems, $\{T\}$ tractions, $\{n\}$ the normal vector and $\{t\}$ the tangent vector to the interface, it can be defined that:

$$\Delta_n = \{\Delta\}.\{n\}$$
$$T_n = \{T\}.\{n\}$$
(1)

and

$$\Delta_t = \{\Delta\}.\{t\}$$
$$T_t = \{T\}.\{t\}$$
(2)

(parenthesis $\{.\}$ are used to represent vectors and brackets $[.]$ to represent second order tensors).A cohesive normal traction arises as a result of the opening according to the phenomenological relations below (for a null tangent opening):

$$T_n = -\frac{\phi_n \Delta_n}{\delta_n^2} \exp\left(-\frac{\Delta_n}{\delta_n}\right)$$
(3)

Equation (3) has a peak value ($\sigma_{máx}$) for a normal opening δ_n . The symbol ϕ_n is the well-known energy fracture per unit area of the crack for mode I opening. Integrating equation (3) in Δ_n, we have the energy dissipated during crack opening (or the area under the curve $T_n x \Delta_n$). For $\Delta_n \gg \delta_n$, this integral is equal to the energy fracture ϕ_n and the cohesive traction T_n is zero, which means rupture of the interface. Replacing $\Delta_n = \delta_n$ in equation (3) we have:

$$\delta_n = \frac{\phi_n}{\exp(1)\sigma_{max}}$$
(4)

The three variables in equation (4) are the fracture parameters for the interface. Then only two of these variables are independent. $\sigma_{máx}$ corresponds to the peak stress on the crack tip and, for ductile (elasto-plastic) materials, its value is around $3 \times \sigma_y$ where σ_y is the yield stress. For pure fragile materials $\sigma_{máx}$ is a function of elastic modulus (*E*) and can variate from *E/10* to *E/100*. (The obvious question that can be raised here is which relation to use for a quasi-fragile material. This question will be addressed in the section 4, where numerical experiments will be done). Figure 1 shows the relation between crack tip stress and crack opening.
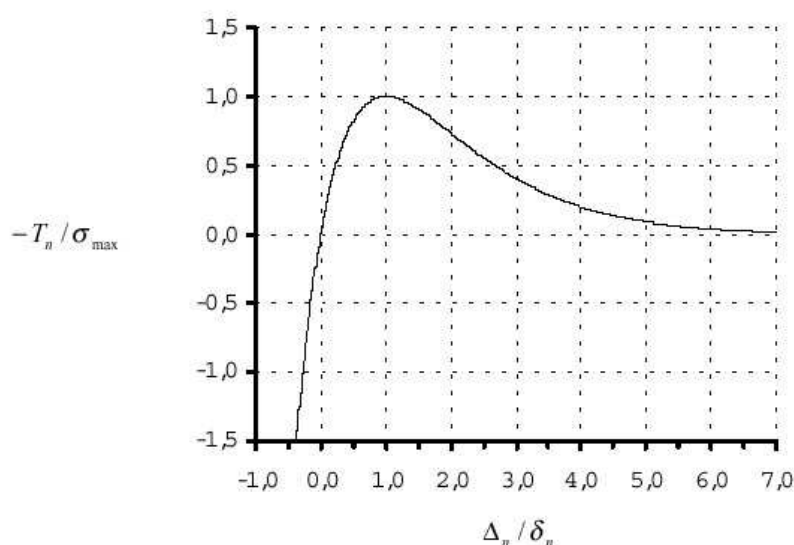
Figure 1: The normalized relationship between normal stress (T_n) and opening (Δ_n).

A cohesive tangent traction is also considered. In this case, considering a null normal opening, we have:

$$T_t = -2\frac{\phi_n \Delta_t}{\delta_n^2}\exp\left(-\frac{\Delta_t^2}{\delta_n^2}\right) \tag{5}$$

In this equation was considered that ϕ_t (the energy fracture per unit area of the crack for mode II) is equal to ϕ_n. T_t and T_n can be considered corotational tractions and then objective related to rigid body rotations.

In this work the concrete is considered an elastic Hookean material. Damage can occur only by separation of interfaces in tension. No compressive damage is considered. The objective Jaumann stress rate $\left[\overset{\triangledown}{\sigma}\right]$ is related to constitutive equation as follows:

$$\left[\overset{\triangledown}{\sigma}\right] = [\Psi]\left[D^e\right] \tag{6}$$

where $[\Psi]$ is the Hooke tensor and $[D^e]$ the rate of deformation. The use of Jaumann stress rate in equation (6), together with corotational cohesive tractions (equations 3 and 5) enable the use of the formulation in large displacements. The Principle of Virtual Work including cohesive tractions, can be written as (body forces are neglected):

$$\int_{\Omega}[\sigma]:\left[\frac{\partial \delta U}{\partial X}\right]dV + \int_{\Gamma_f}\{F\}\{\delta U\}dS + \int_{\Gamma_f}\{T\}\{\delta\Delta\}dS = 0 \tag{7}$$

Constant triangular FE elements are used. The equation above is integrated in each FE volume Ω using one Gauss point, where *{U}* are nodal displacements, *{F}* are prescribed forces on boundary Γ_f. Tractions *{T}* are calculated in all FE faces (except when mentioned otherwise) using four Gauss points; integration is performed over the crack surface Γ_t. An implicit Newton-Raphson scheme is used to solve the corresponding equilibrium equations.

3   FRACTURE PROPERTIES OF CONCRETE

According to Comité Euro-International du Béton (CEB, 1993), G_f (total fracture energy, or ϕ_n plus ϕ_t, in Nm/m) is related to f_{ck}. (characteristic value of concrete compressive strength in MPa) and d_{max} (maximum aggregate size in mm), according to formula below:

$$d_{max} = \frac{G_f}{\left(f_{ck} + 8\right)^{0.7} k} \tag{8}$$

the constant k depends on d_{max} (for instance for d_{max} equal to *4.5, 19* and *25* mm, *k* is equal to *0.0052; 0.0017* and *0.0014* respectively; other values can be interpolated). Observe, then, that the fracture energy depends on two material properties: a stress and a characteristic length. Comparing equation (8) with (4), it can be seen a similarity what suggests that may exist a relation between the characteristic length δ_n and the aggregate size d_{max}.

It should be emphasized that equation (8) is only an attempt to relate concrete most usual properties to fracture. Other ways to calculate fracture properties, can be found in RILEM Recommendations (1990) and considerable different values of these properties are found when comparing to equation (8).

Other relations used by CEB that will be useful here are:

$$E_c = 2.15x10^4 \left(\frac{f_{ck} + 8}{10}\right)^{1/3} \tag{9}$$

where E_c is the tangent elastic modulus of concrete in MPa. Finally,

$$f_{cmt} = 1.4 \left(\frac{f_{ck}}{10}\right)^{2/3} \tag{10}$$

where f_{cmt} is the tensile strength in MPa.

4   NUMERICAL EXPERIMENTATION

We consider here a three point bending beam (or indirect tension), with experimental results obtained from Rots (1988). The tensile strength of the material is f_{cmt}= *2.4 MPa* and Poisson modulus $v = 0.2$. From this properties, using CEB relations of the section 3, is possible to calculate all other relevant properties (we assumed here that maximum aggregate size is $d_{max} = 19$ *mm*).
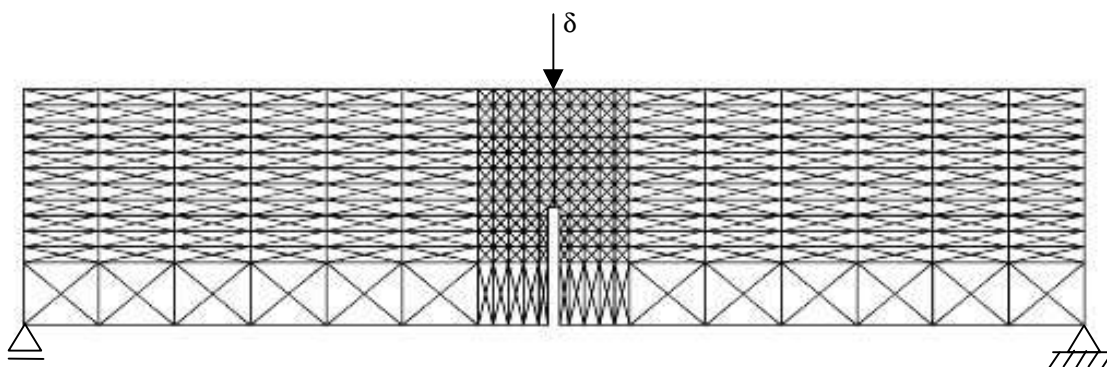
Figure 2: Initial geometry and FE mesh used.

Dimensions of the beam are *450x100x100 mm*. A notch located at the center is *50 mm* long and the opening is *5 mm* (see Figure 2, that shows also FE discretization). A prescribed displacement *(δ)* is applied at the top-center of the beam. The case is considered in plain strain.

To explore the effect of micro-cracking, two situations will be studied. First, cohesive elements (or fracture) will be only considered in the critical section of the beam (central section). Then only one crack is allowed and no micro-cracks outside this plane can exist. Second, a situation where cohesive elements are between all FE of the beam.

4.1 Case with one main crack

The first issue dealing with a quasi-fragile material is to set the maximum stress *(σ_max)* in the crack tip (equation 4). This parameter, together with fracture energy, will define fracture properties according to Xu and Needleman's procedure, defined in section 2. In the Figure 3 a comparison of experimental results with a fragile assumption *(σ_max = E/100)* is shown.
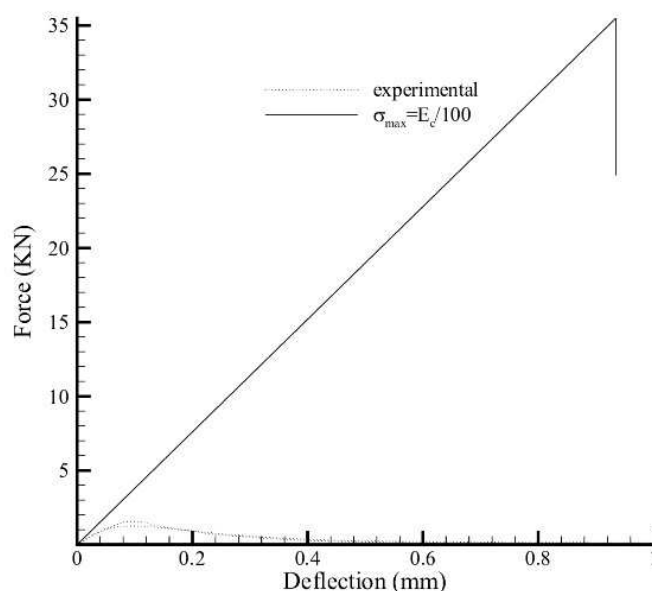
Figure 3: Experimental and numerical load-deflection results. A fragile behavior was assumed for concrete.

It is evident from Figure 3 that the hypothesis of fragile behavior is not adequate to concrete. The force needed to bend the beam is much higher than experimental values and post-peak drop is too abrupt.
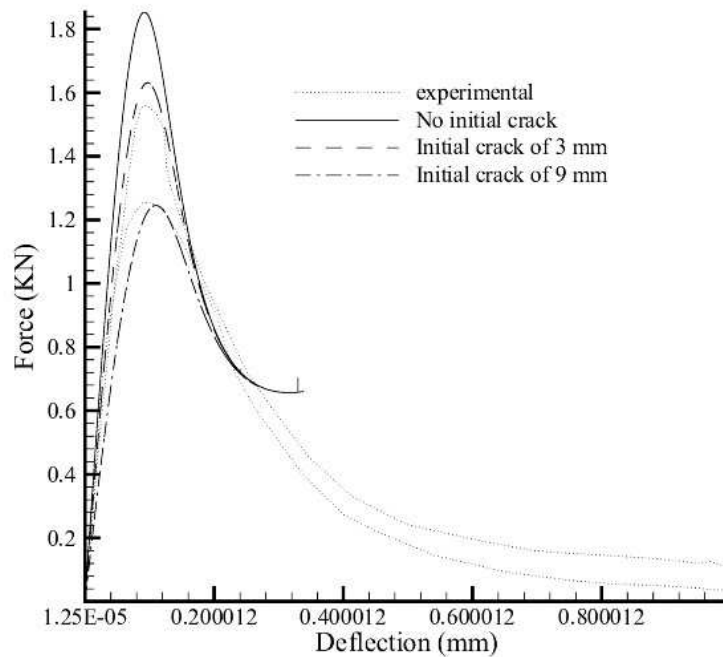
Figure 4: Experimental and numerical load-deflection results. A ductile-like fracture behavior was assumed for concrete $(\sigma_{max}=f_{cmt})$.

Figure 4 shows what happens when $\sigma_{max} = f_{cmt}$. This relation assumes a more ductile-like behavior for concrete, where $\sigma_{max} = f(\sigma_y)$. The results are much more coherent showing that maximum stress in the crack tip of concrete is regulated by f_{cmt} rather than by elastic modulus E. (For deflections of approximately *0.25 mm* only the last cohesive element at the top of the beam was holding it, as shown in Figure 9c. At this point, rupture by compression takes place. As this phenomenon was not considered in this paper, the analyses were aborted). Tijssens et al. (2002) also concluded the same, actually using a value of maximum stress in the crack tip of concrete slightly smaller than f_{cmt}.

In the Figure 4, the notch effect is also explored. If just a square notch is present initially (no initial crack), peak force is greater than experimental. Considering an initial micro-crack in the root of the notch (in the critical plane), then it is possible to fit experimental results. In the results showed in Figure 4, two initial cracks, of *3* and *9 mm*, were considered. This assumption is not crude considering that concrete has a high density of defects in general. However, to assume that (micro) cracks can only be developed in the critical plane is too strong, even considering that, at end of the day, the main crack will follow this plane. This restriction is lifted in the sub-section 4.2 below.

In order to investigate the effect of aggregate size, equation (8) is used to correct fracture energy. Besides the case with $d_{max} = 19\ mm$ (Figure 3 and 4), in Figure 5 is shown what happens with load-deflection curve for $d_{max} \leq 4.5\ mm$ (in this case the aggregate does not change fracture properties of concrete and it can be consider as a mortar) and for a case with $d_{max} = 25\ mm$. It can be seen that aggregate does not change the loading part of the curve and slightly increases load peak and corresponding deflection. Guinea et al. (2002) also observed that aggregates have a noticeable effect only in the unloading part of the curve.
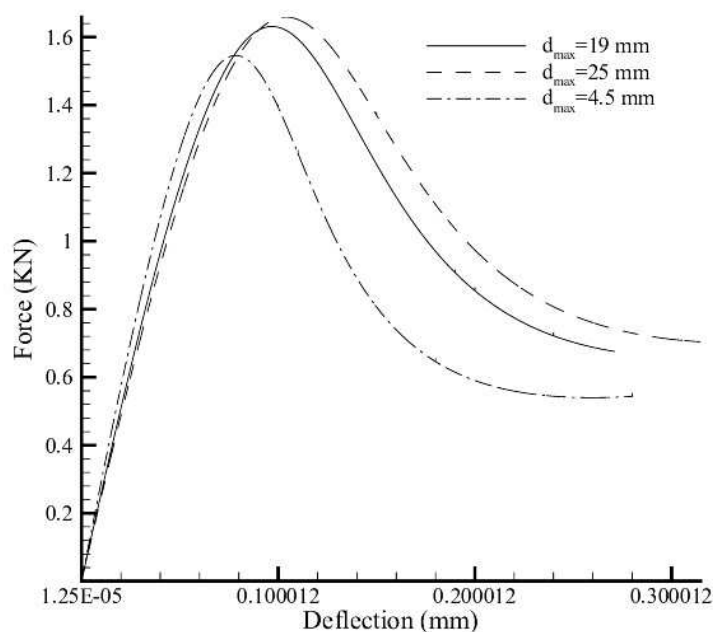
Figure 5: Numerical load-deflection results showing effect of the aggregate size.

It is investigated also the effect of unloading shape part of the cohesive law as follows: the exponential unloading part of the curve is replaced by a linear function, keeping approximately the same area (or fracture energy). The loading part was kept exponential and unchanged, so it will be possible to analyze the unloading effect only. For the case with $d_{max} = 19\ mm$ the resulting cohesive law is shown below in Figure 6.
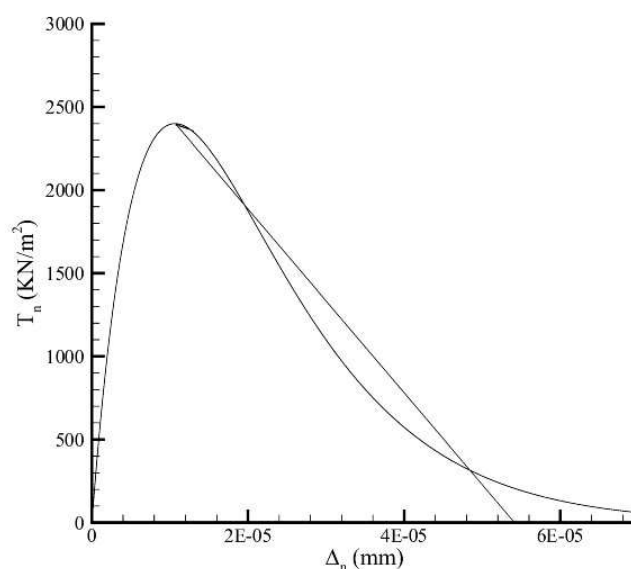
Figure 6: Linear unloading of the cohesive law used in place of exponential unloading. Loading part remains exponential.

Linear unloading load-deflection curve is shown in Figure 7, compared with the same curve for exponential unloading. Peak load and corresponding deflection do not change.

However overall behavior of the beam changes from quasi-fragile to a brittle behavior, with crack propagating suddenly, after peak. Final configuration for the mesh is shown in Figure 7. This behavior indicates that the small tail (Figure 6), eliminated by linearization, has a strong effect in defining a quasi-fragile behavior.
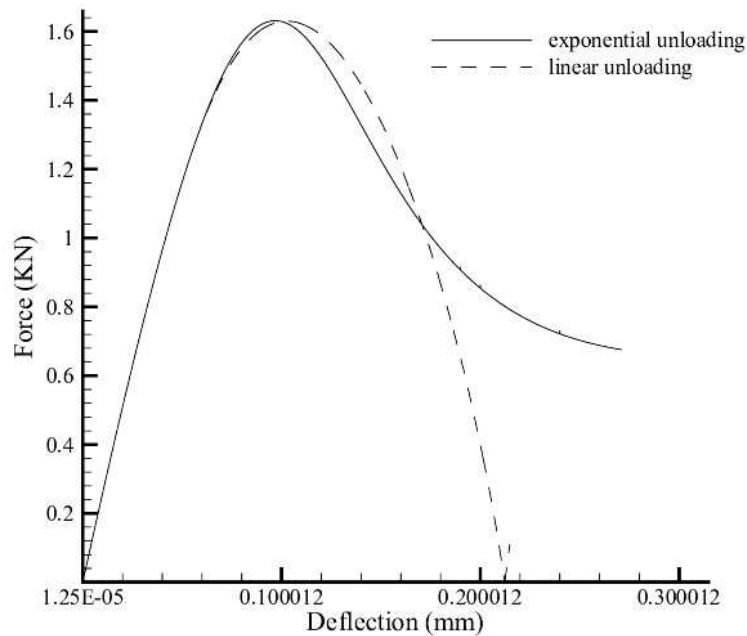
Figure 7: Numerical load-deflection results for two different shapes of unloading part of cohesive law.
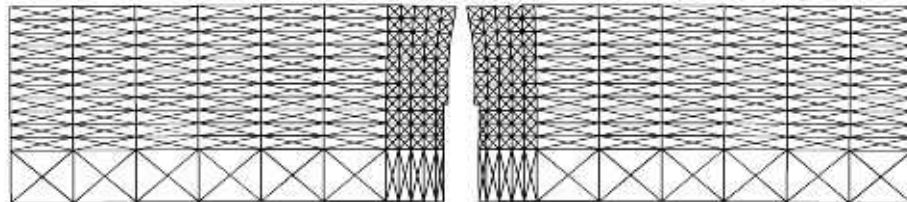
Figure 8: Brittle fracture using linear unloading in the cohesive law

4.2 Case considering micro-cracking

Here fracture interfaces are all over the body. However, for all properties combination used here, main crack ends up always in the critical plane, as expected. This is presented in the sequence of pictures in Figure 9, that shows crack propagation and iso-values of the hidrostatic stress. This is a much more realistic simulation mainly because it considers the development of micro-cracks that open but do not create a macroscopic crack (this is taken into consideration in some limited extent only, due to relatively coarse mesh used). This may have an important hole in mechanical properties of the cracked body, as discussed by Hutchinson (1987) and Ortiz (1988), mainly due to stress release and reduction of elastic modulus.
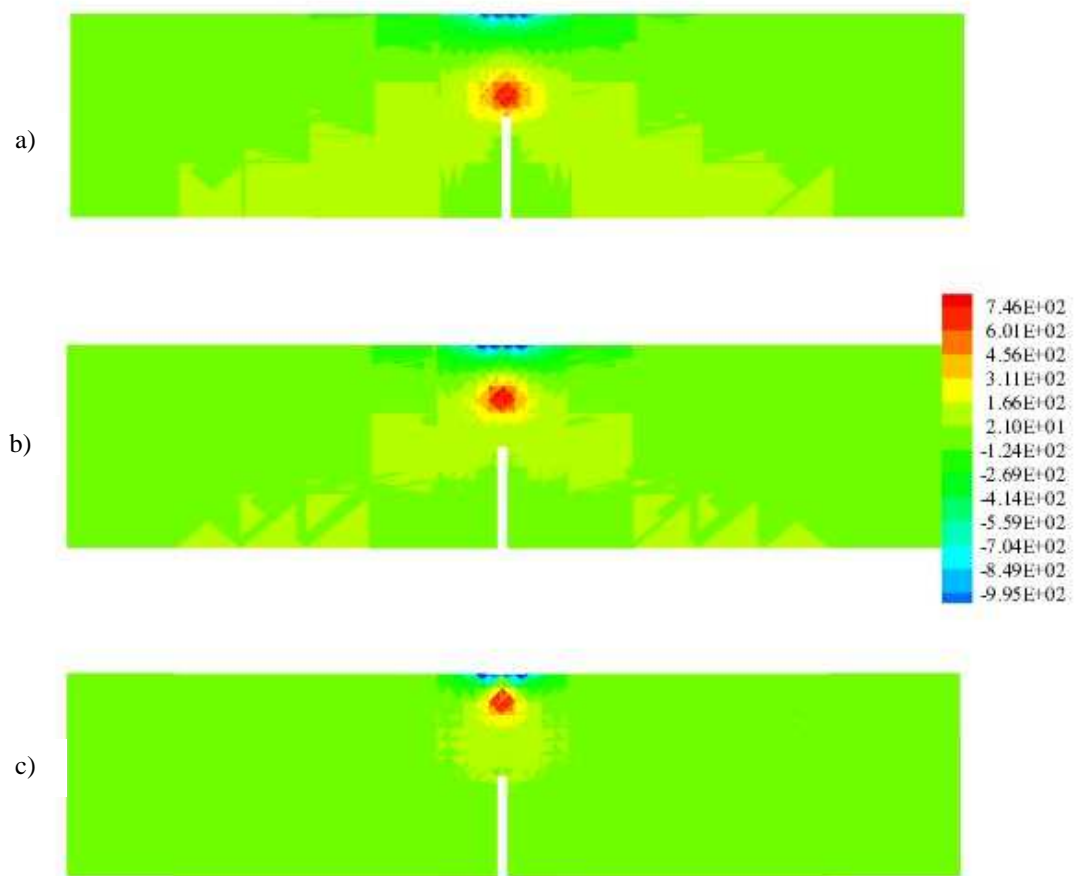
Figure 9: Isovalues of hydrostatic stress when micro-cracking is allowed. Red circles (positive peak of hydrostatic stress) indicate position of the main crack tip, showing that it remains in the critical plane. a) beginning of propagation; b) intermediate configuration; c) final propagation.

Firstly a combination of properties also used in Figure 4 is used here *($\sigma_{max} = f_{ctm}$; $d_{max} = 19mm$*, initial crack of *3 mm* at the root of the notch). Results are shown in Figure 10. The difference in behavior observed here comes only from the fact that now cracks may open all over the body. As expected (see Hutchinson, 1987), a decrease in the force-deflection declivity is evident when compared with the case without micro-cracks (Figure 4). A decrease in the peak load is also observed. Afterwards, a reduction in fracture energy (50%) was tested. It is interesting to remember that, due to linking of fracture properties by equation (4), a reduction in fracture energy, for a constant maximum stress at the crack tip $\sigma_{max} = f_{ctm}$, increases the initial force-deflection declivity. However, the increase in peak load with decrease of fracture energy does not seem reasonable. Actually this trend is the opposite of the shown in Figure 5, where only one crack was considered.
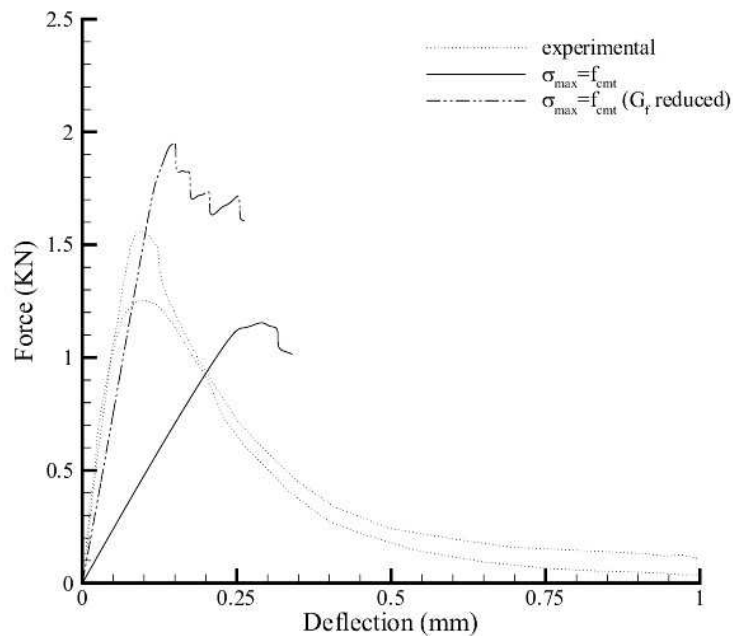
Figure 10: Force-deflection when micro-cracking is allowed. Initial crack of 3mm was used in the root of the notch. A case with reduction of 50% of fracture energy is also shown.

In Figure 11, maximum stress at crack tip was fixed as two times the tensile strength *(σ_{max} = $2f_{ctm}$)*. Two sizes of initial crack at the root notch were used in order to try to fit experimental results. However peak load is always greater than experimental. If initial crack level is again increased, the slope of load-deflection would not fit. It was tried then the linear unloading, keeping all other properties unchanged. As seen in Figure 11, the linear unloading here changes sharply load-deflection curve. Even the peak stress is changed, a modification that does not occur when only one crack is allowed (see Figure 7). It has been reported that the shape of unloading part of stress-opening curve is determinant for overall concrete behavior (Shah et al. 1995; Tjssen et al., 2000). However, it is shown here that this effect is much more intense when micro-cracking is allowed, being more important than maximum crack tip stress. This was also reported in the recent paper by de Borst et al. (2006).
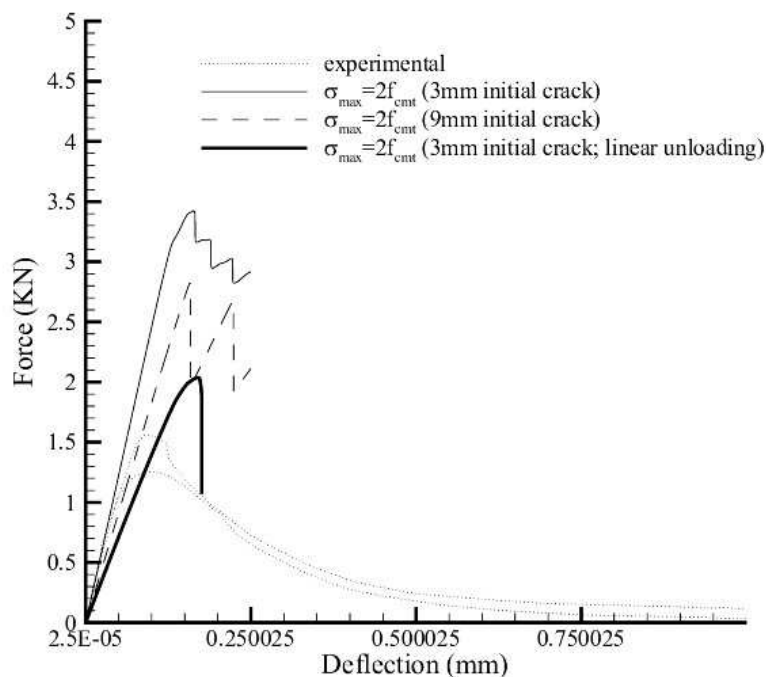
Figure 11: Force-deflection when micro-cracking is allowed. Initial crack of 3mm or 9mm was used in the root of the notch. A case with linear unloading is also shown (exponential unloading is usedwhen not indicated)

5   DISCUSSION AND CONCLUDING REMARKS

In this paper the numerical simulation of the fracture of a concrete beam in three point bending using the Xu and Needleman (1994) exponential cohesive law was analyzed. Experimental load-deflection of the beam was obtained from Rots (1988). It was observed that Xu and Needleman's law works well for concrete when just one crack is allowed, considering that maximum crack tip stress be set equal to the tensile strength of concrete ($\sigma_{max} = f_{ctm}$). It is also able to predict maximum aggregate size effect, that increases peak load and corresponding deflection of the beam at this point. A linearization of the unloading part of the curve does not change peak load, but changes overall behavior of the beam, that passes from quasi-fragile to fragile. The reason is that linearization cuts the final part of the exponential cohesive law, which can be linked with bridging effect of the aggregates (van Mier, 1997). This is one of the key phenomena that give the quasi-fragile behavior to concrete.

However, for a case where micro-cracking is admitted, the use of the exponential law of Xu and Needleman is questionable. This was in fact commented in de Borst et al. (2006). In the same paper is argued that, when micro-cracking is admitted, unloading part of the cohesive law can be more important than maximum crack tip stress. Then, for quasi-fragile material, where micro-cracking is a strong process, the use of a generic cohesive law, such as the one proposed by Xu and Needleman, does not seem adequate. This was actually showed in the present paper. The cohesive law was unable to fit experimental results, and changes in unloading part of the law had a much stronger effect on load-deflection curve of the beam than in the case with only one crack.

It was not the aim of the present work to propose an alternative to model concrete. However, as indicated by Tijssens et al. (2002) and van Mier (1997), a linear unloading does not seem to be adequate to model quasi-fragile materials. The explanation is that softening is

governed by micro-cracking and the rate they are formed is greater after crack tip peak stress. This fact should lead to a sudden drop of the stress-opening relation of the cohesive law. Afterwards a saturation of the process occurs and bridging due to aggregates leads softening process. The drop of the stress-opening relation is then much lower. The exponential law of Xu and Needleman does not fit the initial abrupt drop requirement nor the linear law can model both phenomena described. It seems then that a tri-linear cohesive law can be more adequate to model softening process in concrete. Also the effect of the addition of fibers, that increases concrete toughness basically by bridging, could be also better modeled. The research of an alternative interface law for concrete is ongoing by the present authors.

REFERENCES

R. de Borst, J.J.C. Remmers and A. Needleman. Mesh-independent discrete numerical representations of cohesive-zone models. *Engineering Fracture Mechanics*, 73:160-177, 2006.

N. Chandra, H. Li, C. Shet and H. Ghonem. Some issues in the application of cohesive zone models for metal-ceramic interfaces. *International Journal of Solids and Structures*, 39:2827-2855, 2002.

Comité Euro-international du Béton. CEB-FIP Code Model 1990, *Bulletin d´Information num. 213/214*, Lausane, 1993.

A.A. Guinea, K. el-Sayed, C.G. Rocco, M. Elices and J. Planas. The effect of the bond between the matrix and the aggregates on the cracking mechanics and fracture parameters of concrete. *Cement and Concrete Research*, 32:1961-1970, 2002.

A. Hilleborg, M. Modéer and P.E. Peterson. Analysis of crack formation and crack growth in concrete by means of fracture mechanics and finite elements. *Cement and Concrete Research*, 6:773-782, 1976.

J.W. Hutchinson. Crack tip shielding by micro-cracking in brittle solids. *Acta metallurgica*, 35:1605-1619, 1987.

A.R. Ingraffea, W.H. Gerstle, P. Gergely and V. Sauoma. Fracture mechanics of bond in reinforced concrete. *Journal of Structural Engineering*, 110:871-890, 1984.

M.F. Kaplan. Crack propagation and the fracture of concrete. *Journal of American Institute*, 58:591-610, 1961.

D.J. Naus and J.L. Lott. Fracture Toughness of Portland Cement Concrete. *Journal of American Institute*, 66:481-489, 1969

A. Needleman. Continuum Model for Void Nucleation by inclusion debonding, *Journal of Applied Mechanics,* 54:525-531, 1987.

M. Ortiz. Microcrack coalescence and macroscopic crack growth initiation in brittle solids. *International Journal of Solids and Structures*, 24:231-250, 1988.

P.E. Petersson. Fracture energy of concrete: Practical performance and experimental results. *Cement and Concrete Reserch*, 10:91-101, 1980.

RILEM Draft Recommendation. Determination of fracture parameters (KIC and CTOD) of plain concrete using three-point bend tests. *Material and Structures*, 23:457-460, 1990.

J.G. Rots. *Computational modeling of concrete fracture*. PhD Thesis, Delft University, 1988.

A.C. Santos, J.L.A.O. Souza and T.N. Bittencourt. *Determinação experimental da tenacidade ao fraturamento do concreto em corpos de prova do tipo "short-rod"*. Boletim Técnico Bt

Pef 9807, São Paulo, vol. 1, 1998.

S.P. Shah, S.E. Swartz and C. Ouyang. *Fracture mechanics of concrete: applications of fracture mechanics to concrete, rock and other quasi-brittle material*. Wiley-Interscience publication, 1995.

P.C. Strange and A.H. Bryant. Experimental tests on concrete fracture. *Journal of the Engineering Mechanics Division*, *ASCE*, 105:337-342, 1979

M.G.A.Tijssens, B.L.J. Sluys and E. van der Giessen. Numerical simulation of quasi-brittle fracture using damaging cohesive surface. *European Journal of Mechanics A/Solids* 19:761-779, 2000.

J.G.M. van Mier. *Fracture processes of concrete*. CRC Press, 1997.

X.P. Xu and A. Needleman. A numerical simulation of fast crack growth in brittle solids. *Journal of Mechanics and Physics of Solids*, 42:1397-1434, 1994.